buildings

MDPI

Article

Field Measurement Analysis on Deformation of Adjacent Metro Twin Tunnels Under the Coupling Effect of Servo Supports and Deep Foundation Pit Excavation

Hongyu Tao [1], Shaojun Ma [2], Yucheng Zou [3], Jianfeng Zhu [3], Yongxing He [2], Jiayu Jin [3], Di Qi [4], Yiyi Zheng [5] and Lvjun Tang [6,*]

1 Zhejiang Zheshang Jinji Enterprise Management Co., Ltd., Hangzhou 311200, China; thy73@163.com
2 Zhejiang Province Institute of Architectural Design and Research, Hangzhou 310006, China; mashaojun@zaid.cn (S.M.); heyongxing@ziad.cn (Y.H.)
3 School of Civil Engineering and Architecture, Zhejiang University of Science and Technology, Hangzhou 310023, China; 222402859016@zust.edu.cn (Y.Z.); zhujianfeng@zust.edu.cn (J.Z.); 212402814007@zust.edu.cn (J.J.)
4 Zhejiang Muenster Building Support Technology Co., Ltd., Hangzhou 311022, China; m13588038258@163.com
5 Office of Construction and Campus Planning, Zhejiang University, Hangzhou 310058, China; zhengyiyi@zju.edu.cn
6 College of Civil Engineering and Architecture, Zhejiang University of Water Resources and Electric Power, Hangzhou 310018, China
* Correspondence: tanglj@zuwe.edu.cn

Abstract

To investigate the deformation law of adjacent metro tunnels under the coupling effect of servo supports and deep foundation pit excavation, this study takes an ultra-deep foundation pit adjacent to Hangzhou Metro Line 2 as the research object. A servo support system was adopted for synchronous active loading during excavation, and field monitoring was conducted to analyze the deformation response of existing operating tunnels before and after servo loading. The results indicate that servo loading significantly reduces the rate of increase in tunnel vertical displacement, horizontal displacement, and horizontal relative convergence. It is found that the servo support closest to the tunnel (i.e., the third servo support in the case) exhibits the most prominent control effect—after loading, the vertical displacement rate of the down-line tunnel decreases from −0.04 mm/d to 0 mm/d, and the horizontal displacement rate is reduced by approximately 70%. Moreover, seven days after loading, the horizontal relative convergence rate of the up-line tunnel tends to be 0 mm/d. Servo supports effectively weaken the tunnel's deformation development during critical stages of ultra-deep foundation pit construction, enabling active and precise control of adjacent operating metro tunnels.

Keywords: deep foundation pit; servo loading; metro twin tunnels; field measurement analysis; deformation control

Check for updates

Academic Editor: Erwin Oh

Received: 13 March 2026
Revised: 21 April 2026
Accepted: 1 May 2026
Published: 11 May 2026

1. Introduction

With the rapid development of the urban rail transit and underground space, deep foundation pit construction adjacent to existing metro tunnels has become increasingly prevalent in high-density built-up areas [1–3]. Excavation induces stratum unloading and stress redistribution, which are transmitted to adjacent tunnels via diaphragm walls and soil masses, triggering additional deformations such as vertical displacement, horizontal displacement, and cross-sectional convergence. Given the stringent deformation control criteria for operating metro tunnels, effective mitigation of adjacent tunnel deformation during excavation has emerged as a critical technical challenge in urban underground engineering [4–8].

Extensive studies have been carried out on the mechanism and laws governing tunnel deformation induced by deep foundation pit excavation. Zheng et al. [9] confirmed via a field monitoring analysis that stratum unloading and stress redistribution are the main factors for the additional tunnel deformation. Moreover, the influenced zone expands as the maximum horizontal displacement of the retaining structure increases for a given deflection mode of the retaining structures and a deformation controlling criterion. Peck's ground loss theory [10] and subsequent modifications have demonstrated that the soil displacement field generated by excavation is the primary factor controlling the deformation of adjacent underground structures. Based on continuous field monitoring throughout the entire excavation process of the ultra-deep foundation pit, Tao et al. [11] found that excavation stages dominate the deformation of the tunnel and pipeline. The deformation caused by the excavation stages accounts for more than 60% of the total deformation, which is significantly higher than that induced by the retaining structure construction. This conclusion was validated by Addenbrooke et al. [12] in the metro-adjacent foundation pit studies, indicating that the passive constraints relying solely on the formed retaining structures are insufficient to suppress the continuous excavation disturbances.

From a control perspective, Li et al. [6] proposed a prevention technology to reduce the stratum deformation by optimizing the pressure relief. Mu et al. [13] established a quantitative relationship between soil displacement and longitudinal tunnel deformation via displacement control methods, identifying excavation depth, soil properties, and construction sequence as key factors affecting the magnitude and distribution of the deformation.

Combining numerical simulation and measured data, Su et al. [14] explored the response of an existing metro tunnel horizontal deformation in soft clay to the capsuled expansion technique. Zhao et al. [15] further noted that excavation-induced stress path changes cause significant additional tunnel deformation, with vertical displacement typically exceeding horizontal displacement and exhibiting distinct stage characteristics.

Engineering practices have verified these laws through field measurements. Gu et al. [16] conducted systematic monitoring of tunnel deformation during deep foundation pit construction adjacent to double-line metro tunnels, finding that vertical settlement and horizontal displacement increase significantly during critical excavation stages—even conventional support and construction control measures may not eliminate non-negligible additional deformation. However, most existing research and engineering measures focus on the static support and passive control, such as enhancing retaining structure stiffness, densifying supports, and optimizing construction processes, lacking real-time active regulation capabilities for tunnel deformation during excavation. In recent years, with the advancement of information-based construction and active control concepts, servo support technology has been gradually applied in the complex deep foundation pit projects. By conducting numerical simulations and engineering practice measurements, Sun et al. [17] demonstrated that servo supports dynamically adjust the axial force to adapt to the excavation conditions, effectively suppressing retaining structure displacement. Wang et al. [18] reported the field evidence showing that the servo support system effectively reduced the lateral displacement of the retaining wall. The servo jacks also introduced a localized inflection point and shifted the displacement profile upward, thereby altering the bending behavior of the retaining structure. Wei et al. [19] confirmed that active loading during excavation reduces cumulative stratum deformation and improves foundation pit stability. Nevertheless, existing studies primarily focus on the effects on retaining structures and the surrounding strata, with limited field measurements on deformation responses of adjacent operating metro tunnels under the synchronous action of servo supports and excavation, especially the lack of a systematic comparative analysis of multiple tunnel deformation indicators over short time scales before and after servo loading.

To compensate for the above deficiencies, this study implements synchronous active loading using a servo support system during the excavation of a deep foundation pit adjacent to metro tunnels. Based on the field monitoring data, it compares tunnel deformation responses in key stages before and after servo loading, focusing on variations in vertical displacement, horizontal displacement, and horizontal convergence. The weakening effect of servo supports on tunnel deformation during critical excavation stages is quantitatively evaluated, verifying their active control capability in practical engineering. The results provide a valid reference for a support system design and the controlled construction of deep foundation pits adjacent to existing metro tunnels.

2. Project Overview

2.1. Project Introduction

This project is located in Xiaoshan District, Hangzhou, China, involving the construction of a four-story basement with a frame-shear wall structure and cast-in-place pile foundations. The foundation pit covers an area of approximately 14,900 m^2 with a perimeter of 540 m, within which the A1 foundation pit occupies about 2620 m^2. It is located adjacent to the 6.2 m-diameter shield tunnel of Hangzhou Metro Line 2 between Qianjiang Road Station and Qianjiang Century City Station. The outer diameter of the shield tunnel (D) is 6.2 m, and the segment thickness is 0.35 m. The segments are made of C50 concrete with a standard ring width of 1.2 m, and they are in the northeast of the foundation pit. The minimum horizontal distance between the foundation pit and the tunnel is 11.1 m (i.e., 1.8‰D) (Figure 1). The excavation depth is 9.50 m for the two-story basement, 17.60 m for the general four-story basement, and up to 19.70 m at the tower location. As the foundation pit is very close to the operating metro tunnel, strict control of excavation-induced tunnel deformation and compliance with metro protection specifications are prioritized [20–22].

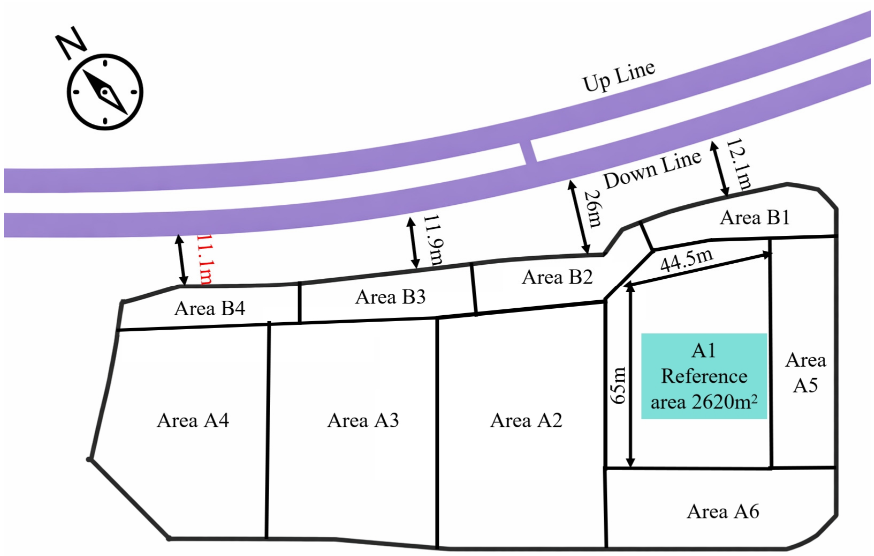

Figure 1. Schematic diagram of the relative position between the tunnel and the foundation pit.

A1 is the first foundation pit excavated in this project. In the following sections, analyses are primarily focused on the deformation of the tunnels induced by the construction of foundation pit A1, and a brief introduction to A1 is presented as follows. Excavation of

Panel A1 reaches a depth of 19.2 m, with corresponding plan dimensions of approximately 44.5 m in length and 65 m in width. On the north side of foundation pit A1, the retaining structure is designed as a diaphragm wall. The wall has a thickness of 0.8 m and a length of 37.9 m. On the east, west, and south sides of foundation pit A1, the retaining structures are designed as pile walls. Each cast-in-place pile has a diameter of 1.0 m and a length of 33.2 m, with a center-to-center spacing of 1.2 m between the adjacent piles. The waterproof curtain external to the pile walls is constructed with triaxial cement-soil mixing piles. These cement-soil mixing piles have a diameter of 0.85 m and a length of 21.6 m, with a center-to-center spacing of 0.6 m between the adjacent piles. Foundation pit A1 is equipped with four concrete truss supports. The first-level support is non-servo concrete support, while the other three are servo concrete supports. From top to bottom, the vertical distances from the top of each support to the top of the diaphragm wall or piles are 0 m, 4.7 m, 8.7 m, and 12.5 m, respectively.

2.2. Environmental Conditions Around the Foundation Pit

The project's surrounding environment is complex (Figure 2), with adjacent metro tunnels, urban roads, and temporary facilities imposing strict deformation control requirements. The east side of the pit is 11.1 m from the metro tunnel (a high-sensitivity zone), with the nearest road edge 23 m from the pit; the tunnel structure is highly sensitive to construction disturbances [23,24], which makes this side a core constraint for deformation control. The south side adjoins a planned road and vacant land, with only 1.6 m between the pit's inner edge and the red line, resulting in narrow construction space that imposes higher requirements for the retaining system design and construction organization. The west side is 2.5 m from an urban main road, where vehicle loads and vibrations may affect pit stability, making it a key monitoring and controlling section. The north side is 23.5 m from another urban main road, with traffic loads and potential construction disturbances requiring inclusion in support system safety assessments. Additionally, the metro tunnel is 15–20 m below ground, with temporary facilities (e.g., finished product stacking areas with 6 kPa additional load) above—such concentrated loads are prone to inducing additional tunnel stress [25], necessitating strict control over layout, stacking height, and duration. Due to the superposition of these factors, high-precision deformation monitoring and servo-active support technology are essential for real-time deformation regulation.

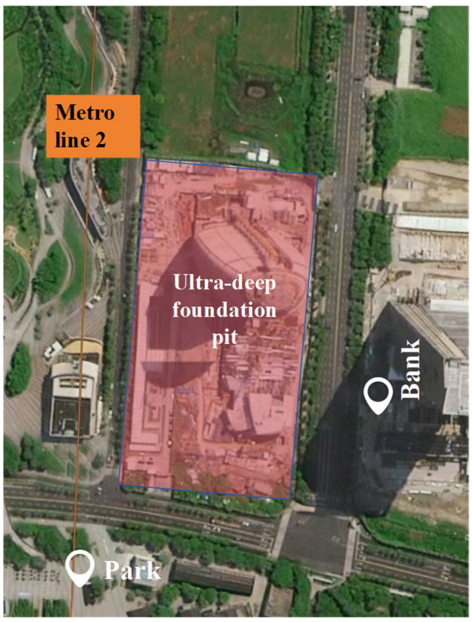

Figure 2. Schematic diagram of the surrounding environment of the foundation pit.

https://doi.org/10.3390/buildings16101904

2.3. Engineering Geology and Hydrogeology

The site is located in the Qiantang River fluvial-marine accumulation plain, characterized by a layered stratum consisting of miscellaneous fill, clayey silty soil, sandy silty soil, sandy silt with interlayers of fine sand, mucky silty clay, silty sand, and round gravel (Figure 3). The physical and mechanical parameters of the stratum are shown in Table 1. The hydrogeology of the site is relatively complex. The phreatic water is in the shallow layers, and the water level burial depth is 1.2–2.8 m according to the seasonal variation. While the waterproof curtain has some flaws, it is prone to seepage during excavation. The confined water is in the deep layers (i.e., the silty sand and the round gravel), and the elevation of the total water head for the confined water is about −8.5 m. While the overlying cohesive soil exerts a water-resisting effect, the confined water impacting the pit bottom safety requires attention during deep excavation.

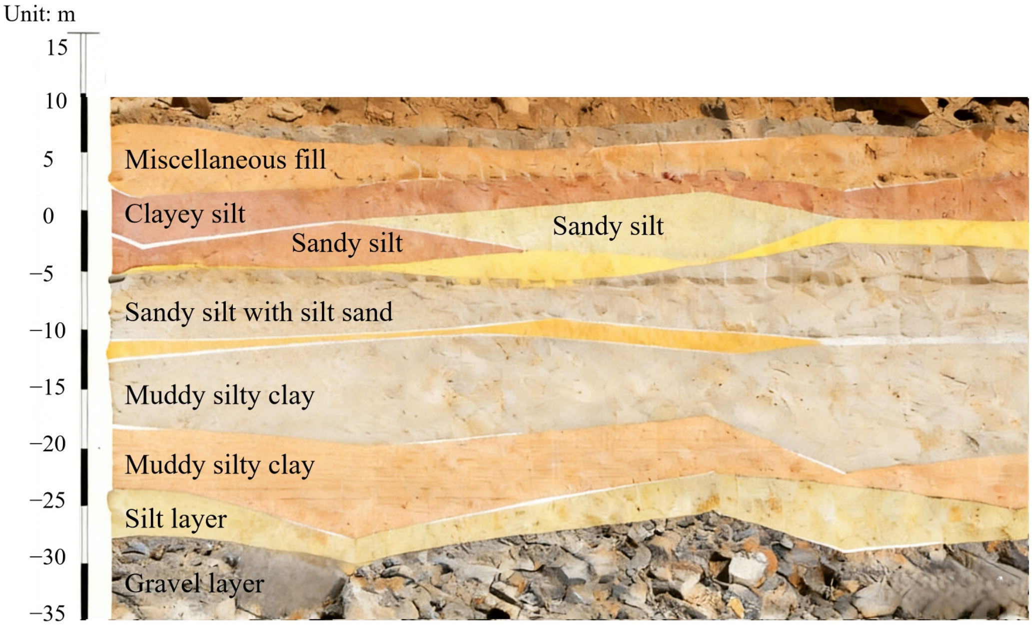

Figure 3. Engineering geological profile.

Table 1. Physical and mechanical parameters of the stratum.

Stratum	Density (kN/m^3)	Cohesion (kpa)	Friction Angle (°)	SPT Blow Count
miscellaneous fill	18.5	10	12	/
clayey silt	18.3	8.0	20.0	12.3
sandy silt	19.1	5.5	28.0	11.6
sandy silt with interlayers of fine sand	19.3	6.0	26.0	11.8
mucky silty clay	17.6	13.0	9.0	/
silty sand	19.2	3	33.0	16.2
round gravel	20	3	38.0	/

3. Overview of Servo Active Support Technology

3.1. Basic Concept of Servo Active Support

The servo active support system incorporates active axial force adjustment into traditional concrete supports, integrating servo jacks and control devices to dynamically regulate axial force and actively control the deformation of the retaining structure and adjacent infrastructure (Figure 4). The concrete double-purlin servo system comprises the outer purlins (bearing and transferring water-soil pressure), the inner purlins (key force transfer component), the concrete support piers, the concrete support beams, and the servo compensation devices. When the servosystem is shut down, the lateral water-soil pressure is transmitted sequentially through outer purlins, support piers, inner purlins, and concrete support beams. When the servosystem is activated, the jack-generated axial force is first transmitted to the outer and inner purlins, and then the force is transmitted to the retaining structure and support beams. The servo system provides the pre-deformation reverse restraint. On one hand, it avoids sudden stress increases and improves concentration. On the other hand, it maintains the axial force within a reasonable range to suppress the lateral displacement and enhance the foundation pit stability. The system can also be combined with basement floor slabs to form a servo support replacement system (Figure 5), enabling the stable transfer of the support force to the main structure, avoiding excessive deformation of the foundation pit during the support replacement and demolition.

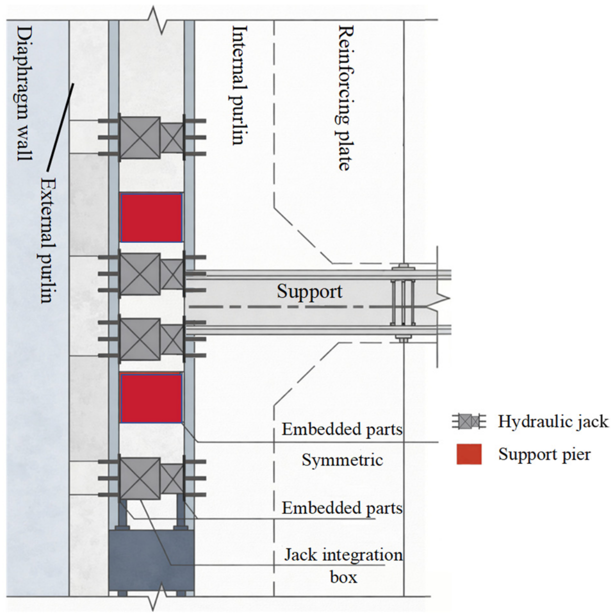

Figure 4. Schematic diagram of the servo system for concrete double-purlin supports.

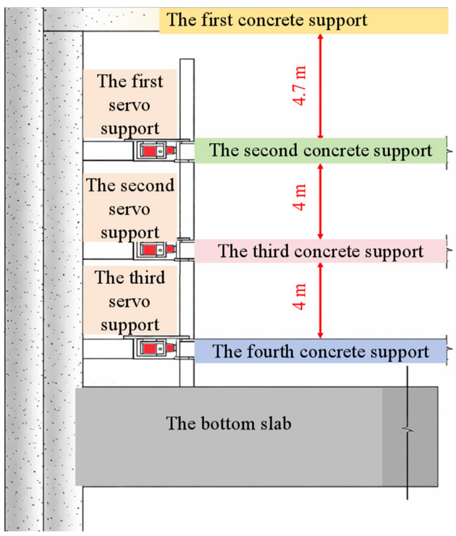

Figure 5. Schematic diagram of support replacement application for concrete double-purlin supports.

3.2. Working Principle of Servo Active Support

Centered on the coordinated control of the retaining structure displacement and support axial force (Figure 6), the system operates as follows: it monitors support axial force and retaining structure displacement in real time via sensors mounted on the support members, with automatic unloading and alarming for the excessive axial force, and automatic loading for the insufficient axial force. When the measured displacement approaches the control limits, the system dynamically optimizes axial force settings based on the displacement responses. Thus, the coupled axial force-displacement regulation is realized. The initial pressure-holding control is based on the designed axial force, with periodic revisions using monitoring data to match actual stress states and avoid axial force attenuation from concrete deformation or temperature effects. During pressurization, potential separation between inner and outer purlins (Figure 7) is a normal response, but requires monitoring via crack distance meters and vernier calipers. Post-loading and high-strength non-shrinkage grouting are used to fill gaps, restoring force transmission integrity and ensuring long-term support stability.

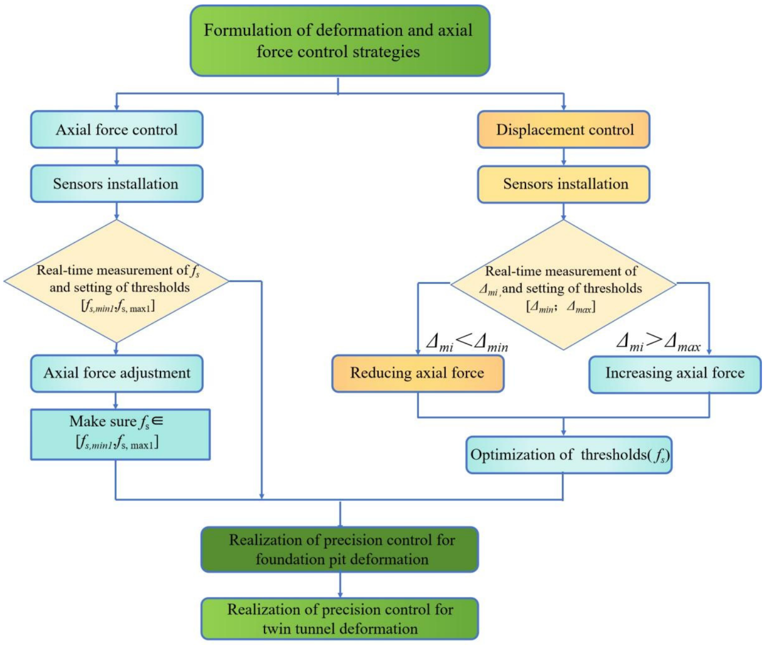

Figure 6. Flow chart of the servo system for concrete double-purlin supports.

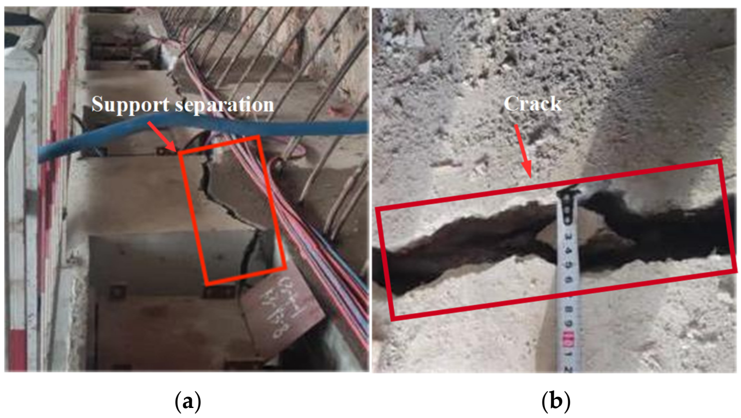

Figure 7. Schematic diagram of cracks in double-purlin servo supports: (**a**) Support separation gap; (**b**) Crack measurement.

3.3. Construction Process of Ultra-Deep Foundation Pit Based on Servo Support

The construction process of pit A1 (Table 2) involves eleven key steps: the initial concrete support installation to form a primary horizontal support frame, followed by layered excavation, sequential installation, and active loading of servo supports (second–fourth). Then, the "support installation → excavation → servo loading" cycle is repeated until the fourth servo support is installed and loaded. Lastly, the bottom concrete slab is poured to form the bottom support.

Table 2. Construction steps of pit A1 excavation based on servo support action.

Process	Construction Content
S1	Installation of the first concrete support
S2	Excavation of the first soil layer
S3	Installation of the second concrete support and the first servo support
S4	Axial loading of the first servo support
S5	Excavation of the second soil layer
S6	Installation of the third concrete support and the second servo support
S7	Axial loading of the second servo support
S8	Excavation of the third soil layer
S9	Installation of the fourth concrete support and the third servo support
S10	Axial loading of the third servo support
S11	Pouring of the bottom slab

4. Construction Monitoring Scheme of Ultra-Deep Foundation Pit Based on Servo Support

To investigate excavation-induced tunnel deformation, monitoring sections were arranged at equal intervals in the up-line S340–S400 and down-line X340–X400 tunnel sections (Figure 8), with a horizontal spacing of 30 m. Monitoring was conducted on a daily basis, with one set of data collected every 24 h, and the monitoring frequency was intensified during critical stages (e.g., excavation and servo loading). In the event of monitoring point damage, immediate replacement and data continuity correction were implemented to ensure the integrity of the dataset. Outliers were identified and filtered through consistency checks and trend analysis. Early warning thresholds for tunnel deformation, including vertical displacement, horizontal displacement, and horizontal convergence, were conservatively set at ±3 mm based on design specifications, engineering experience, and deformation control requirements, thereby ensuring the reliability and safety of the monitoring system. Each was equipped with a reflective prism array (Figure 9): Prism 1 and prism 4 monitor horizontal convergence, while prism 2 and prism 3 monitor the vertical and horizontal deformation. A Leica TM50 total station was used for high-precision 3D coordinate measurements, obtaining millimeter-level deformation via multi-period coordinate tracking. Continuous monitoring was conducted, with data used to analyze vertical displacement (S_v), horizontal displacement (S_h), and horizontal relative convergence (D_t) to evaluate impacts on tunnel structural safety.

https://doi.org/10.3390/buildings16101904

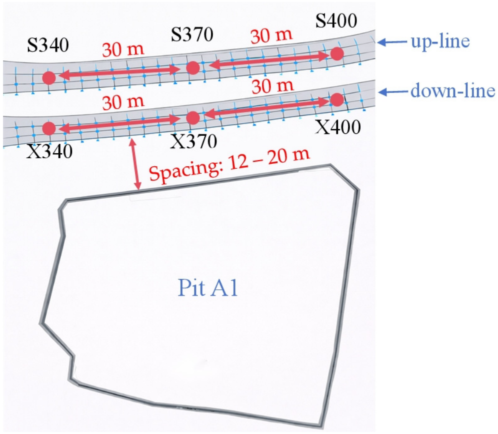

Figure 8. Schematic diagram of measuring points on the up-line and down-line of the tunnel.

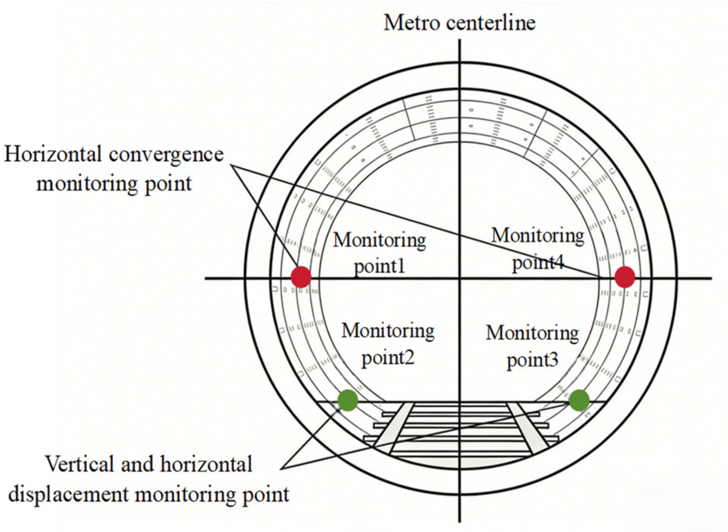

Figure 9. Layout of prisms at the monitoring section.

5. Field Measurement Analysis of Deformation of Adjacent Metro Tunnels (Up-Line/Down-Line)

Pit A1 was excavated from 8 March to 5 August 2023, with a maximum depth of 19.3 m. The first support is a conventional concrete support, and the second–fourth are servo concrete supports with active pre-loading before subsequent layer excavation; the fifth support is a conventional concrete bottom slab. The second–fourth supports (working conditions S4, S7, S10) each contain 20 jacks per layer, with the servo load values per meter being 849 kN/m, 920 kN/m, and 990 kN/m (Table 3), respectively, and increasing the burial depth to counteract rising lateral soil pressure. Each jack has a maximum loading capacity of 3500 kN and a maximum stroke of 0.2 m. Monitoring data were analyzed using a "7-days before loading—7-days after loading" symmetric time window to isolate servo effects from long-term excavation trends. This short-term window is considered appropriate, as deformation monitoring data are typically treated as time-series data, and short-duration intervals are commonly adopted to capture the immediate response of surrounding structures to construction disturbances [26,27]. Moreover, the 7-day window ensures sufficient data points under daily monitoring frequency, providing a balance between sensitivity to short-term changes and robustness against data fluctuations. Deformation rates 7 days before (δ_7) and after (η_7) loading were calculated for the representative up-line/down-line measuring point 370 (Equations (1) and (2)), where x is the loading-day deformation value, and x_{a7}/x_{b7} are deformation values 7 days before/after loading.

$$\delta_7 = (x - x_{a7})/7 \quad (1)$$

$$\eta_7 = (x_{b7} - x)/7 \quad (2)$$

Table 3. Application time and load magnitude of servo supports.

Step	Date	Process	Axial Load Applied to Each Support per Meter (kN/m)
1	27 April 2023	S4	849
2	2 June 2023	S7	920
3	3 July 2023	S10	990

5.1. Field Measurement Analysis of Tunnel Vertical Displacement

During the foundation pit excavation and servo loading process, soil unloading will induce vertical heave or settlement of adjacent tunnels. Vertical displacement can directly reflect the response degree of the tunnel structure due to the disturbance from the foundation pit excavation, which is also a key indicator for evaluating the control effect of the servo supports.

Five monitoring points are selected for the up-line and down-line tunnels, respectively. The variation curves of tunnel vertical displacement are shown in Figure 10, where the positive vertical displacement Sv represents heave, while the negative vertical displacement represents settlement. The reading values of all measuring points are zero on the day of foundation pit excavation. The distribution rules of vertical displacement at each measuring point are as follows:

(1) The displacement curves of both the up-line and down-line tunnels show the spatial characteristic that "the vertical displacement reaches the peak value near the measuring point 355, and gradually decreases towards both ends along the line".

(2) The vertical displacement of the up-line tunnel is generally in the range of −0.4–0.4 mm, with little difference in the curve shapes of the three working conditions, and the maximum value of approximately 0.4 mm occurs in the S7 stage. The vertical displacement amplitude of the down-line tunnel is slightly larger, ranging from −0.8 to 0.8 mm overall, and the maximum value of about 0.8 mm appears at XCJ355 in the S4 stage.

(3) From the perspective of safety, the maximum vertical displacement of the tunnel is only 0.8 mm, which is significantly less than the vertical displacement early warning index (i.e., 10 mm) commonly used in the protection monitoring of existing urban rail transit structures [28]. Therefore, it can be determined that the vertical deformation of the tunnel under various working conditions is within a reasonable and safe control range.

To further identify the regulatory effect of servo support loading on the development process of vertical deformation, this study compares the vertical displacement rates of measuring point 370 before and after loading under various support conditions (see Figure 11). In the subsequent context, $\delta_{7\mathrm{u,v}}$ and $\eta_{7\mathrm{u,v}}$ represent the vertical displacement rates of the up-line 7 days before and after loading, while $\delta_{7\mathrm{d,v}}$, $\eta_{7\mathrm{d,v}}$ denote the vertical displacement rates of the down-line tunnels 7 days before and after loading. The variation patterns of the vertical displacement rate are as follows:

(1) For the up-line tunnel in the S4 stage, both $\delta_{7\mathrm{u,v}}$ and $\eta_{7\mathrm{u,v}}$ are 0.01 mm/d, with no significant difference before and after loading. However, with the increase of support loading depth in the S7 stage, $\delta_{7\mathrm{u,v}}$ remains 0.01 mm/d, while $\eta_{7\mathrm{u,v}}$ decreases to 0. In the S10 stage, $\delta_{7\mathrm{u,v}}$ of the up-line tunnel is −0.04 mm/d, and $\eta_{7\mathrm{u,v}}$ drops to 0 mm/d, indicating that the control effect of deep servo support loading is significantly better than that of the shallow support stage.

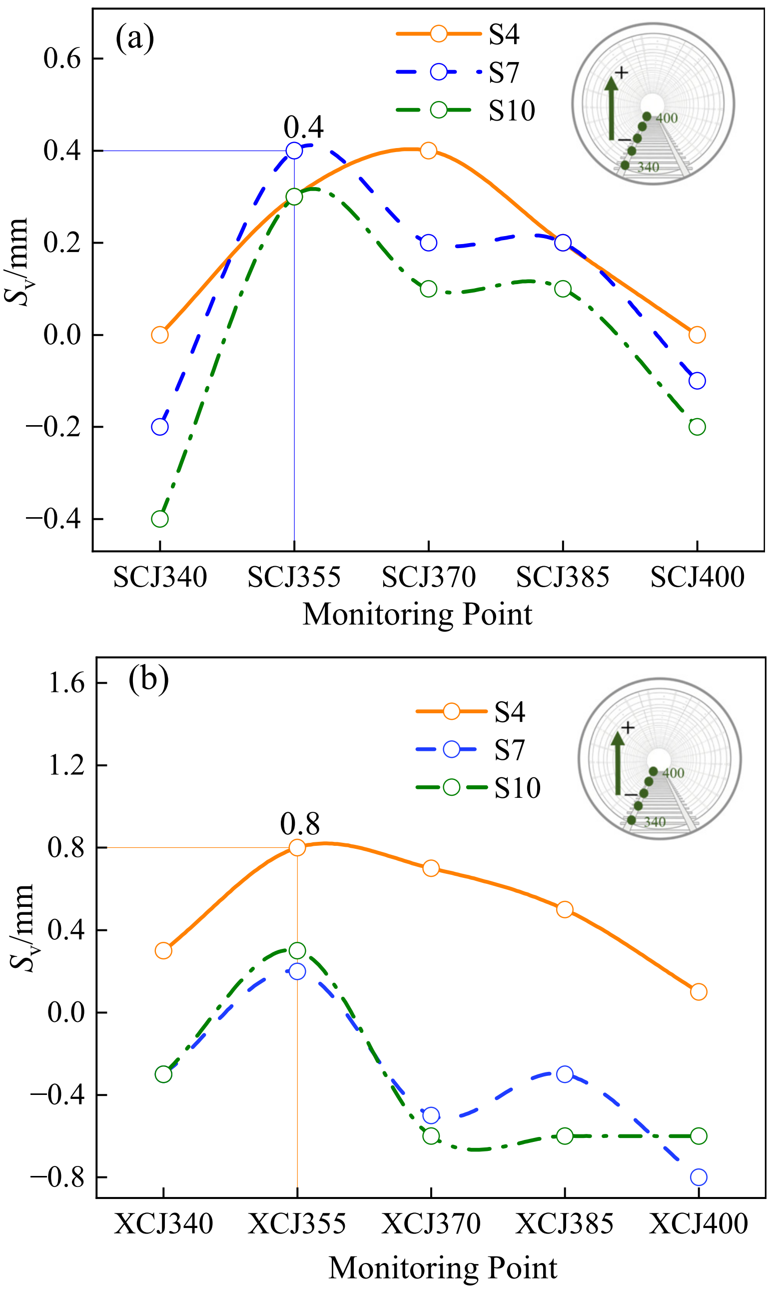

Figure 10. Vertical displacement curves of tunnel measuring points under various working conditions: (**a**) up-line; (**b**) down-line.

(2) The down-line tunnel shows a more significant response to servo support loading. In the S4 stage, $\delta_{7d,v}$ is 0.11 mm/d, and $\eta_{7d,v}$ decreases to 0.10 mm/d, with a small variation range. In the S7 stage, the vertical displacement rate decreases from −0.07 mm/d before loading to −0.03 mm/d after loading, a reduction of approximately 57%, indicating that loading has an obvious inhibitory effect. In the S10 stage, $\delta_{7d,v}$ is −0.04 mm/d, and $\eta_{7d,v}$ drops to 0 mm/d, effectively suppressing the development rate of vertical deformation of the tunnel.

(3) The control effect of servo supports on tunnel vertical deformation is mainly reflected in reducing the deformation development rate. Shallow loading has a limited effect on the vertical displacement rate. After the loading of the fourth servo support, the vertical displacement of both the up-line and down-line tunnels is effectively suppressed, and the vertical response of the tunnel enters a controlled and stable state.

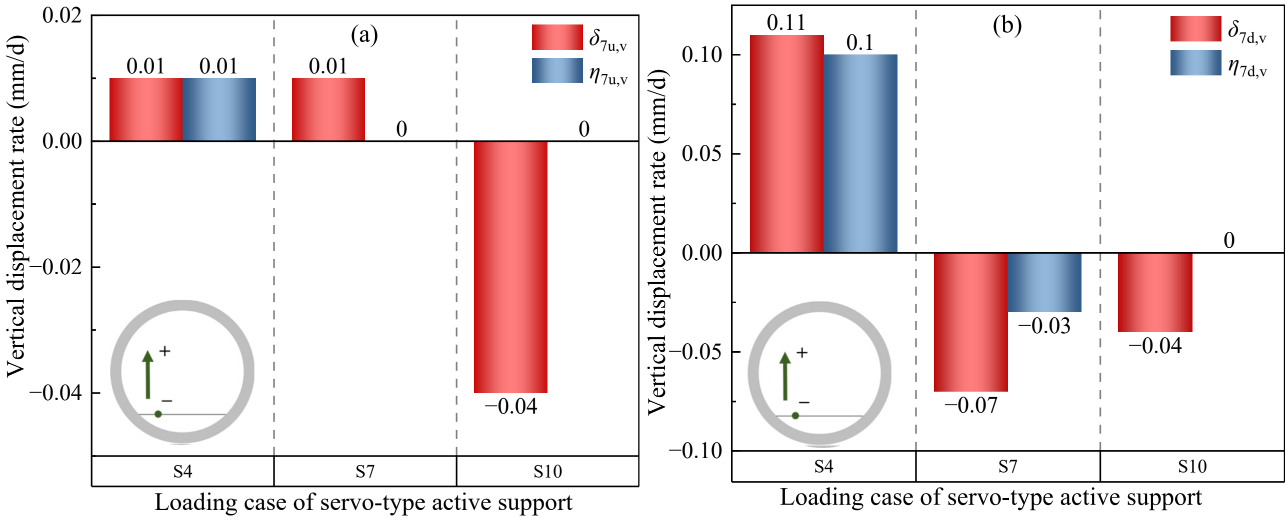

Figure 11. Tunnel vertical displacement rate changes before and after each support loading: (**a**) up-line; (**b**) down-line.

5.2. Field Measurement Analysis of Tunnel Horizontal Displacement

Figure 12 shows the variation curves of tunnel horizontal displacement Sh. It should be noted that a positive value indicates displacement towards the foundation pit, while a negative value indicates displacement away from the foundation pit. The horizontal displacement of all measuring points is zero before foundation pit excavation. The distribution rules of horizontal displacement at each measuring point are as follows:

(1) Under the condition of servo support loading, both the up-line and down-line tunnels mainly displace horizontally towards the foundation pit.

(2) The Sh of the up-line tunnel generally shows a trend of gradual increase with the increase of measuring point number. Among them, the horizontal displacement of SSP400 reaches the maximum value under various working conditions, reaching approximately 0.5‰D (i.e., 3.0 mm) in the S10 loading stage, while the displacement amplitude of the SSP340 measuring point far from the foundation pit is small.

(3) The horizontal displacement amplitude of the down-line tunnel is significantly larger than that of the up-line tunnel. The peak horizontal displacement of the middle measuring point XSP370 of the foundation pit reaches 0.75‰D (i.e.,4.5 mm), which is 1.5 times that of the maximum horizontal displacement of the up-line tunnel. Moreover, the down-line tunnel is closer to the foundation pit and is more strongly disturbed by foundation pit construction.

Figure 13 compares the horizontal displacement rates of measuring point 370 7 days before and after loading under different working conditions. In the subsequent context, $\delta_{7u,h}$ and $\eta_{7u,h}$ represent the horizontal displacement rates of the up-line 7 days before and after loading, while $\delta_{7d,h}$ and $\eta_{7d,h}$ denote the horizontal displacement rates of the down-line tunnels 7 days before and after loading. The variation patterns of the horizontal displacement rate are as follows:

(1) For the up-line tunnel, the effect is not obvious in the shallow support loading stage. While in the S10 stage, the horizontal displacement rate 7 days before loading is 0.04 mm/d, and it decreases to 0.01 mm/d 7 days after loading, a reduction of about 75%, indicating that the deep servo support effectively suppresses the continuous horizontal displacement of the up-line tunnel towards the foundation pit.

(2) The down-line tunnel exhibits a more significant response to servo support loading. In the S10 stage, $\delta_{7d,h}$ before loading reaches 0.07 mm/d, and $\eta_{7d,h}$ after loading

drops to −0.03 mm/d, showing a trend of deformation transformation from "continuous displacement towards the foundation pit" to "rebound adjustment".

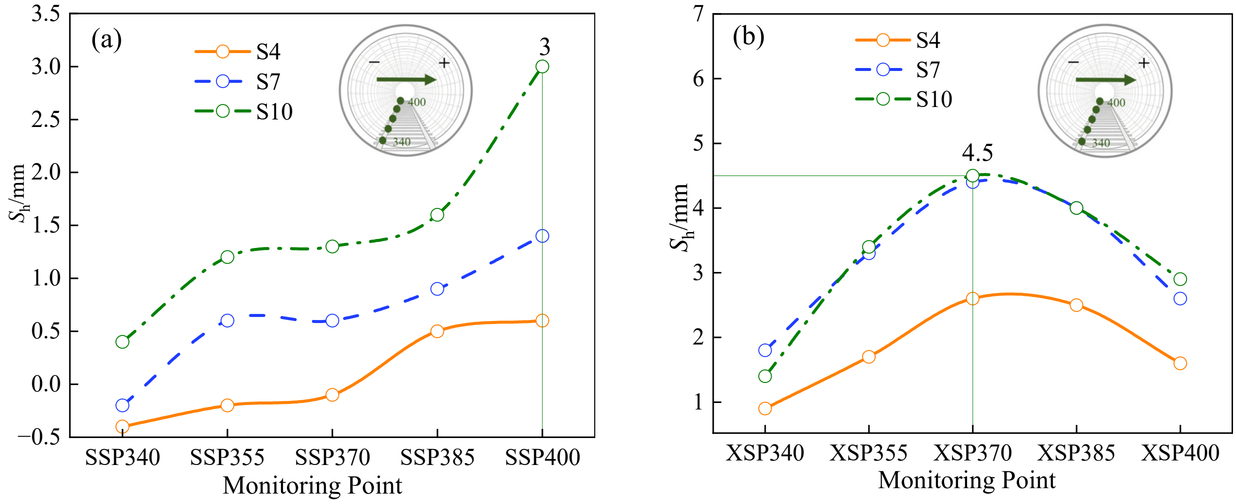

Figure 12. Horizontal displacement of the tunnel during the loading of each servo active support: (**a**) up-line; (**b**) down-line.

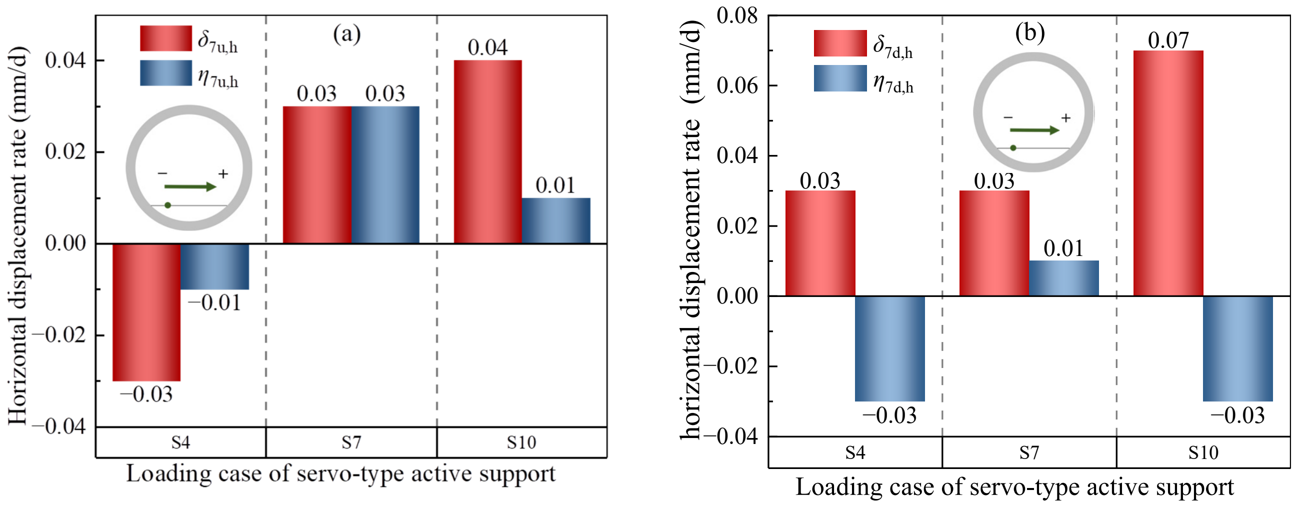

Figure 13. Tunnel horizontal displacement rate changes before and after each support loading: (**a**) up-line; (**b**) down-line.

Although the overall horizontal displacement of the tunnel during foundation pit excavation is mainly towards the foundation pit, servo supports can significantly reduce the development rate of horizontal displacement. In addition, deep servo supports can effectively limit the further inward displacement of the retaining structure, bringing the development of tunnel horizontal displacement into a stable state.

5.3. Field Measurement Analysis of Tunnel Horizontal Convergence

Figure 14 shows the variation trend of tunnel horizontal convergence D_t (i.e., the relative horizontal displacement between two points in the segments at the same elevation of the tunnel center) under various servo loading conditions. It should be mentioned that a positive value indicates a decrease in horizontal diameter (i.e., inward convergence), while a negative value indicates an increase in horizontal diameter (i.e., outward convergence). It can be seen from Figure 14 that:

(1) During the whole process of synchronous implementation of foundation pit excavation and servo support, the horizontal convergence values of both the up-line and down-line tunnels are positive in general, indicating that the tunnels are in a state of lateral compression.

(2) The horizontal convergence values of each measuring point on the up-line tunnel are generally small, mainly distributed in the range of 0.3–0.9 mm, and show a slow accumulation characteristic with the advancement of construction.

(3) The horizontal convergence amplitude of the down-line tunnel is significantly larger than that of the up-line tunnel, showing an "M" shape. The convergence value of measuring point XSL385 is the most prominent, with the maximum value exceeding 2 mm in the period of the last servo loading (i.e., S10). This indicates that the down-line tunnel, being closer to the foundation pit, is more susceptible to the combined influence of displacement of the retaining structure and lateral soil pressure concentration, and its lateral compression effect is significantly stronger than that of the up-line tunnel.

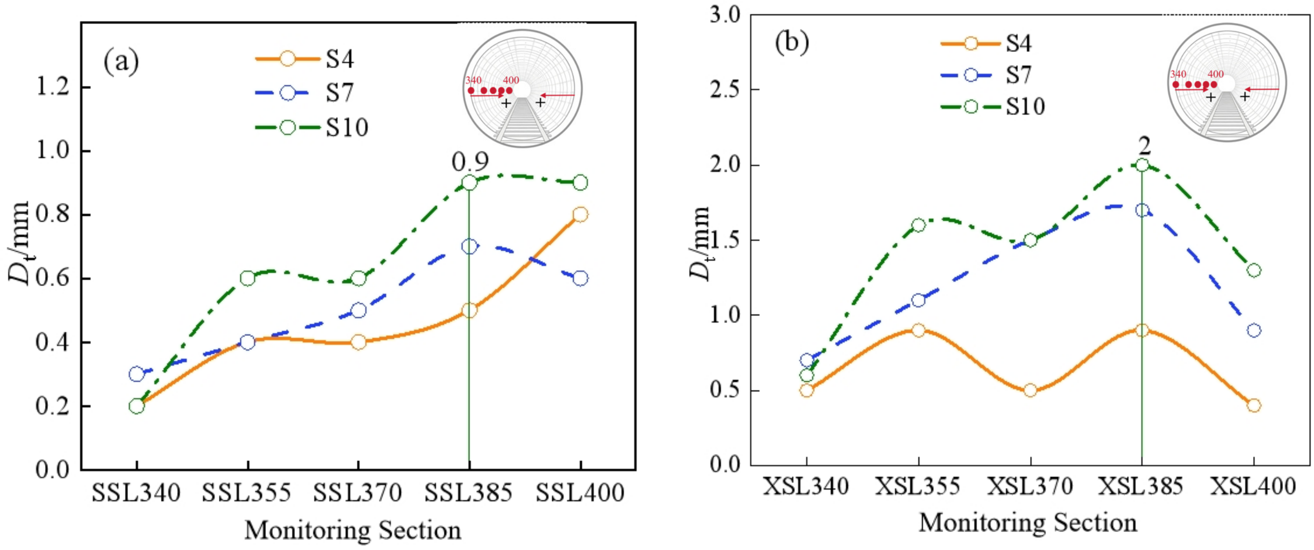

Figure 14. Horizontal convergence of the tunnel during the loading of each servo active support: (**a**) up-line; (**b**) down-line.

Measuring point 370 is also selected for the analysis, where $\delta_{7u,t}$ and $\eta_{7u,t}$ represent the horizontal convergence rates of the up-line 7 days before and after loading, while $\delta_{7d,t}$ and $\eta_{7d,t}$ denote the horizontal convergence rates of the down-line 7 days before and after loading. It can be seen from Figure 15 that:

(1) For the up-line tunnel in the S4 stage, the horizontal convergence rate $\delta_{7u,t}$ within 7 days before loading is 0.03 mm/d, and it turns to −0.01 mm/d 7 days after loading, which weakens the development trend of tunnel lateral compression in this stage. Subsequently, in the third and fourth support loading stages, the post-loading rate decreases to 0 mm/d, and the stress state tends to be stable.

(2) For the down-line tunnel in the S4 stage, the rates before and after loading are both 0.01 mm/d, indicating that the shallow support has a limited immediate regulatory effect on the lateral compression of the down-line tunnel. However, after the loading of the second servo support, the rate changes from 0.01 mm/d to −0.01 mm/d, indicating that the support begins to exert an inhibitory effect on convergence accumulation. In the third servo support loading stage, $\delta_{7d,t}$ reaches 0.04 mm/d, and $\eta_{7d,t}$ decreases to 0.03 mm/d, with its development rate being reduced.

(3) The horizontal convergence of the tunnel generally shows the characteristics of continuous compression and gradual accumulation during foundation pit excavation.

Servo supports function by reducing the convergence development rate and delaying the accumulation process. In the third servo support loading stage (i.e., S10), the convergence rate of the up-line tunnel decreases to 0 mm/d, and the rate of the down-line tunnel is reduced. Its active axial force can effectively weaken the transmission intensity of the lateral soil pressure to the tunnel, thereby improving the lateral stress state of the tunnel and slowing down convergence accumulation.

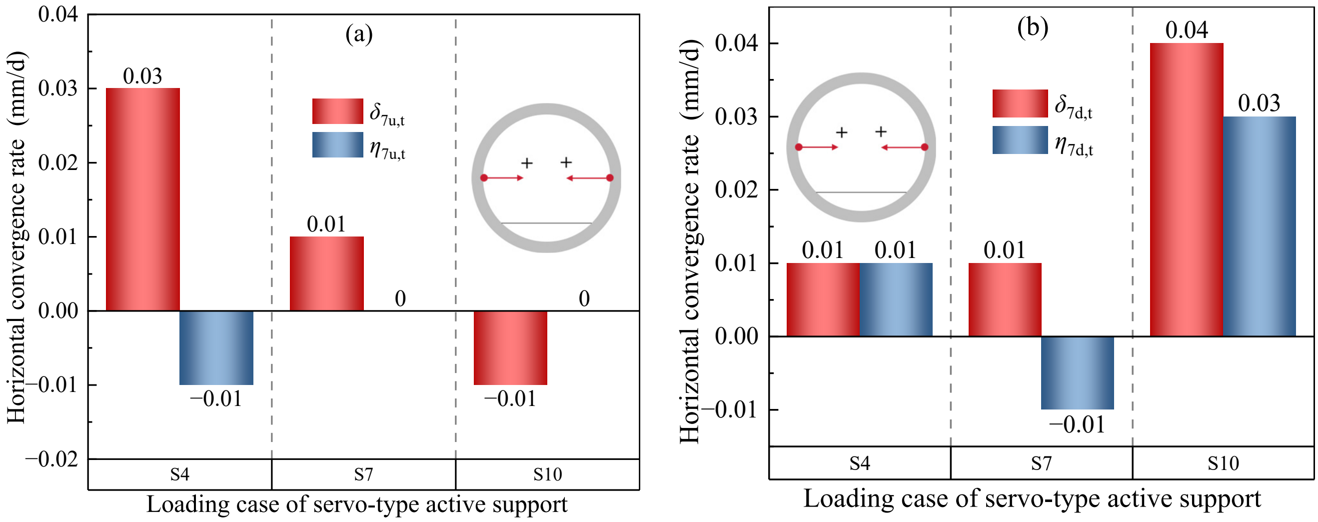

Figure 15. Horizontal convergence rate changes of the tunnel before and after each support loading: (**a**) up-line; (**b**) down-line.

5.4. Mechanism Analysis

The above field measurement results show that under the construction mode of synchronous implementation of servo supports and foundation pit excavation, the vertical displacement, horizontal displacement, and horizontal relative convergence of the adjacent metro tunnels are all effectively controlled, and the deformation development rates are significantly lower than those of engineering cases characterized by "implementing servo loading after the completion of foundation pit excavation" in the existing literature [29–31]. However, after the application of servo supports, the overall displacement of the tunnel is still mainly "towards the foundation pit". The main mechanism is that the servo supports prop up the retaining structure in advance, reduces the inward movement of soil towards the pit, and transforms the tunnel deformation from "continuous increase" to "slowing down or even stabilizing". As shown in Figure 16, the effects of servo loading in each stage can be explained as follows:

(1) When the second servo support is loaded (see Figure 16a), its position is obliquely above the tunnel and far away from the tunnel, mainly serving to suppress the inward displacement of the upper part of the retaining structure. At this time, the impact caused by foundation pit excavation will still propagate to the deep part, and the tunnel may still undergo a certain degree of displacement and deformation. Therefore, the direct control effect of the second servo loading on tunnel deformation is relatively limited, and its main role is to establish the support system and lay the foundation for subsequent deep control.

(2) The loading position of the third servo support is deeper. After loading, the inward displacement trend of the retaining structure is further restricted, and the inward squeezing of soil towards the pit is also weakened. Therefore, the development rate of the tunnel's horizontal displacement will decrease significantly, and the vertical displacement will be more likely to stabilize. At this stage, the control effect of the servo supports on tunnel deformation begins to be significantly reflected.

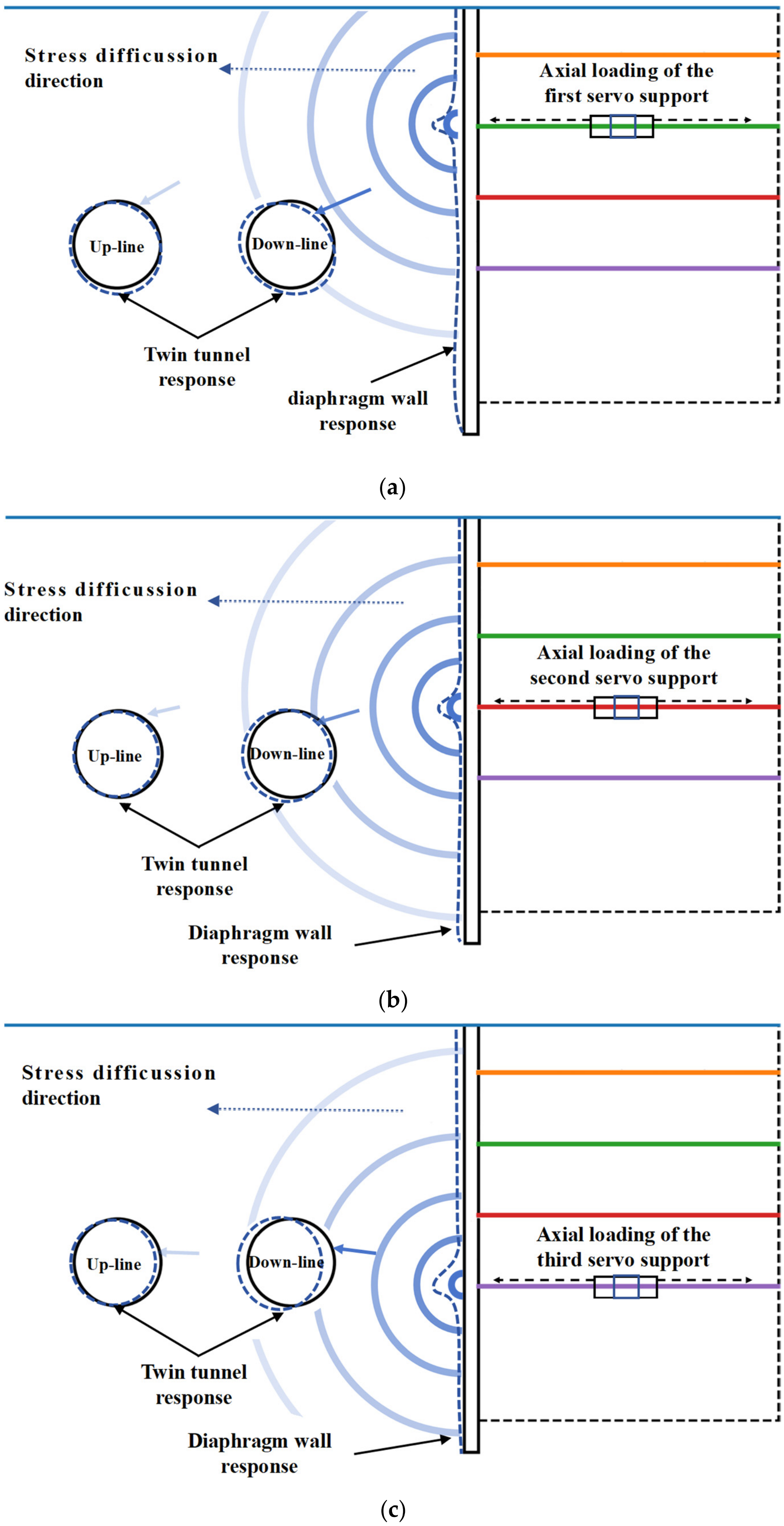

Figure 16. Deformation mechanism diagram of adjacent tunnels under servo-driven active loading: (**a**) S4; (**b**) S7; and (**c**) S10.

(3) When the fourth servo support is loaded, the support depth is close to the tunnel burial depth, which has the most direct and effective inhibitory effect on the deep inward

displacement of the retaining structure. Since tunnel deformation is often mainly caused by deep soil unloading and lateral movement, the servo supports need to apply a larger axial force under the influence of deep soil pressure. After deep servo loading, the impact transmitted to the tunnel is greatly reduced, the growth rate of tunnel horizontal displacement will slow down significantly, and even a local "rebound adjustment" trend will appear. The advantage of the fourth loading lies in its control over the "most critical source of deep deformation", bringing the tunnel deformation into a more stable and controlled state, which is the fundamental reason for its obvious control effect.

In summary, the second servo loading mainly plays an early constraint role, while the stress transmission distance is long, resulting in a weak impact on the tunnel. The third servo loading begins to significantly reduce the tunnel deformation growth rate. The fourth servo loading, with the closest loading path to the tunnel, can more effectively restrict the transmission of deep lateral displacement to the tunnel and achieve the best comprehensive control effect.

6. Conclusions

This study investigates the deformation characteristics of the double-line metro tunnels during the excavation of the adjacent foundation pit. Based on the monitoring data, the tunnel displacement and convergence under the coupling effect of servo supports loading and deep foundation pit excavation were systematically analyzed. The mechanism for controlling tunnel displacement through the active loading of servo supports was also proposed. The main conclusions are summarized as follows:

(1) Under the condition of "synchronous implementation of excavation—servo support" in pit A1, the vertical displacement of the adjacent double-line tunnels is generally in the range of −0.8–0.8 mm, with a maximum value of only 0.8 mm, which is significantly less than the vertical displacement early warning index of existing tunnels, indicating that the vertical deformation is within a safe and controllable range.

(2) The overall horizontal displacement of the tunnel is mainly towards the foundation pit, and the response of the down-line tunnel is significantly stronger. The maximum horizontal displacement of the up-line tunnel occurs at the easternmost side, reaching 0.5‰D in the S10 stage. The peak value of the down-line tunnel is at the position closest to A1 in the middle of the foundation pit, reaching 0.75‰D, which is about 1.5 times that of the corresponding position of the up-line tunnel, indicating that the down-line tunnel is more sensitive to construction disturbances.

(3) The horizontal convergence of the tunnel is positive under all working conditions, showing continuous lateral compression accumulation. The convergence value of the up-line tunnel is mainly 0.3–0.9 mm, while that of the down-line tunnel is larger and concentrated in the middle section, with the maximum value exceeding 2 mm in the later construction period.

(4) The deformation rate changes in the "7 days before loading—7 days after loading" time window indicate that the primary function of the servo support system is to mitigate the rate of tunnel deformation, thereby restraining excessive displacement during excavation, and the effect of deep loading is the most prominent. After the loading of the third servo support, the horizontal displacement rate of the up-line tunnel decreases by about 75%. The horizontal displacement of the down-line tunnel changes from 0.07 mm/d to −0.03 mm/d, transforming from continuous lateral displacement to rebound adjustment. The vertical displacement rate of both lines decreases to 0, and the deformation enters a stable and controlled state.

(5) Due to the third servo support loading depth being closest to the tunnel burial depth, it has the most direct inhibitory effect on the deep lateral displacement. Moreover, it

achieves the best comprehensive control effect on the double-line tunnels, which is reflected in the significant reduction of the growth rates of horizontal displacement and convergence, and the transformation of tunnel deformation from "continuous accumulation" to "significant deceleration and stabilization".

It is important to mention that, compared to the traditional non-servo support system, although the servo support system increases the partial cost due to the servo system itself, the overall cost of the whole retaining structure is significantly reduced by adopting the servo system. For this project, in order to meet the deformation control requirements, the thickness of the concrete diaphragm wall was optimized from 1.0 m to 0.8 m by adopting the servo support system, resulting in a cost reduction of approximately 20% compared to the traditional support systems. In addition, the concrete consumption of the retaining structure has been effectively reduced, which reasonably lowers carbon emissions and brings considerable energy-saving benefits. Furthermore, the servo system can be dismantled immediately when the underground structure has been completed. After routine maintenance, the dismantled servo system can be reused, resulting in relatively low long-term maintenance costs.

It should also be noted that the deformation behavior of the adjacent metro twin tunnels under the coupled effects of servo support and deep excavation is governed by complex soil-structure interaction mechanisms. This study primarily focuses on the short-term deformation characteristics induced during excavation and synchronous servo loading. However, further investigations are required to establish a comprehensive mechanical model of the retaining structure–soil–tunnel interaction system, to elucidate the spatial distribution characteristics of deformation over the entire tunnel section, and to reveal the long-term deformation evolution after project completion. In particular, future research will provide long-term monitoring data, statistical analysis, and analytical insights into the stabilization process of tunnel deformation over time.

Author Contributions: All authors contributed to the conception and design of the study. Writing—original draft preparation and data curation were performed by H.T. and Y.Z. (Yucheng Zou). Supervision, writing—review and editing, and funding acquisition were performed by J.Z. Methodology was developed by S.M. and L.T. Resources were provided by Y.H. and D.Q. Conceptualization and investigation were carried out by J.J. and Y.Z. (Yiyi Zheng). All authors have read and agreed to the published version of the manuscript.

Funding: This work was supported by the Joint Fund of Zhejiang Provincial Natural Science Foundation of China (LGEY26E090013), Zhejiang Construction Scientific Research Project (2023K110), Hangzhou Construction Scientific Research Project (2023056).

Data Availability Statement: All data used during this study appear in the submitted article.

Conflicts of Interest: Author Hongyu Tao was employed by Zhejiang Zheshang Jinji Enterprise Management Co., Ltd. Author Shaojun Ma and Yongxing He were employed by Zhejiang Province Institute of Architectural Design and Research. Author Di Qi was employed by Zhejiang Muenster Building Support Technology Co., Ltd. The remaining authors declare that the research was conducted in the absence of any commercial or financial relationships that could be construed as a potential conflict of interest.

References

1. Zhao, Y.R.; Chen, X.S.; Hu, B.; Huang, L.P.; Lu, G.H.; Yao, H.L. Automatic monitoring and control of excavation disturbance of an ultra-deep foundation pit extremely adjacent to metro tunnels. *Tunn. Undergr. Space Technol.* **2023**, *142*, 105445. [CrossRef]
2. Hamdhan, I.N.; Alamsyah, R. Evaluation of soil deformation due to complex construction of deep excavation and microtunneling to repair underground pipe leakage. *IOP Conf. Ser. Earth Environ. Sci.* **2025**, *1514*, 012001. [CrossRef]
3. Kar, D.; Ghosh, A. Effect of deep excavation on adjacent shield tunnel using nonlinear Pasternak soil model. *Geotech. Geol. Eng.* **2025**, *43*, 287. [CrossRef]

4. Lai, F.W.; Lu, D.C.; Tschuchnigg, F.; Schweiger, H.; Shiau, J.; Huang, M.; Zhou, X. Effectiveness of protective strategies for mitigating deep excavation effects on nearby existing tunnels. *Int. J. Geomech.* **2026**, *26*, 04025316. [CrossRef]
5. Li, Q.; Yang, S.L.; Yue, H.; Kong, D.Z. Study on Caving Characteristics of Roof and Floor and Law of Ground Pressure Behavior in Near-Vertical Coal Seams Mining: A Three-Dimensional Similarity Simulation Experiment. *Rock Mech. Rock Eng.* **2026**, *59*, 2155–2188. [CrossRef]
6. Li, Q.; Yang, S.L.; Song, Y.H.; Wei, W.J.; Zhang, J. Study on Deformation Mechanism and Control Technology of Rock Pillar in Near-Vertical Coal Seams Mining. *Bull. Eng. Geol. Environ.* **2026**, *85*, 89. [CrossRef]
7. Le, T.N.; Le, T.T.; Lai, V.Q. A numerical investigation on reducing the effects of deep excavation on adjacent metro lines using jet grouting. *Transp. Infrastruct. Geotechnol.* **2025**, *12*, 43. [CrossRef]
8. Ter-Martirosyan, A.Z.; Kivliuk, V.P.; Isaev, I.O.; Rud, V. Projected effects of a deep excavation pit on the existing metro tunnel and findings of geotechnical monitoring: A comparative analysis. *Buildings* **2023**, *13*, 1320. [CrossRef]
9. Zheng, G.; Du, Y.M.; Diao, Y.; Deng, X.; Zhu, G.P.; Zhang, L.M. Influenced zones for deformation of existing tunnels adjacent to excavations. *Chin. J. Geotech. Eng.* **2016**, *38*, 599–612. [CrossRef]
10. Peck, R.B. Deep excavations and tunneling in soft ground. In *Proceedings of the 7th International Conference on Soil Mechanics and Foundation Engineering*; State of the Art Report; Sociedad Mexicana de Mecánica de Suelos: Mexico City, Mexico, 1969; pp. 225–290.
11. Tao, Y.L.; Chen, K.; Zhu, J.F.; Gong, X.N.; Yu, Z.Y. Monitoring analysis on the surrounding deformation of super deep foundation pit during the whole construction process in urban dense area. *Chin. J. Undergr. Space Eng.* **2024**, *20*, 969–977. [CrossRef]
12. Addenbrooke, T.I.; Potts, D.M. Twin tunnel construction-ground movements and lining behaviour. In Proceedings of the International Symposium on Geotechnical Aspects of Underground Construction in Soft Ground, London, UK, 15–17 April 1996; pp. 441–446.
13. Mu, L.L.; Zhang, P.Y.; Shi, Z.H.; Zhu, M.X.; Gu, Z.W. Predicting longitudinal tunnel deformation due to deep excavation-induced ground movement. *Tunn. Undergr. Space Technol.* **2023**, *131*, 104793. [CrossRef]
14. Su, Y.M.; Zheng, G.; Diao, Y.; Li, Z.W.; Peng, J.; Jia, J.W.; Huang, J.Y.; Huang, K.Q. Horizontal Deformation of a Tunnel Controlled by Capsuled Expansion Technique in Soft Clay: Field Trial and Numerical Analysis. *Int. J. Geomech.* **2025**, *25*, 04024324. [CrossRef]
15. Zhao, X.; Wang, H.X.; Li, Z.W.; Dai, G.L.; Yin, Z.W.; Cao, S.N.; Zhou, J.L. Numerical study on the deformation of tunnels by excavation of foundation pit adjacent to the subway. *Appl. Sci.* **2022**, *12*, 4752. [CrossRef]
16. Gu, X.W.; Yi, Z.H.; Wang, Z.; Chang, K. Influences of excavation of deep foundation pits on deformation of adjacent double-line subway tunnels through measurement analysis. *Chin. J. Geotech. Eng.* **2023**, *45*, 214–219. [CrossRef]
17. Sun, J.C.; Sheng, J.C.; Wang, Z.; Yao, Z.W. Investigating the strength of foundation pit bracing structure with active control of axial force. *J. Ground Improv.* **2023**, *5*, 133–143. [CrossRef]
18. Wang, S.C.; Xu, L.; Zhang, X.H.; Long, L.Y.; Zhuang, X.Y. Development and field analysis of a novel servo concrete bracing system for deep foundation pit excavation. *Buildings* **2024**, *14*, 1674. [CrossRef]
19. Wei, G.; Feng, F.F.; Zhu, J.X.; Li, J.; Zhang, X.J.; Chen, C.L. Measurement and analysis of deep foundation pit excavation of adjacent shield tunnel with servo steel support. *J. Nat. Disasters* **2023**, *32*, 93–104. [CrossRef]
20. Rakoczy, A.; Wilk, S.; Jones, M.C. *Research Report and Findings: Specifications and Guidelines for Rail Tunnel Design, Construction, Maintenance, and Rehabilitation*; United States Department of Transportation, Federal Transit Administration: Washington, DC, USA, 2022.
21. Lohar, G.K.; Kumar, A.; Roy, N. Numerical assessment of time-dependent deformation of a road tunnel—A case study. *Transp. Infrastruct. Geotechnol.* **2024**, *11*, 447–469. [CrossRef]
22. Maes, K.; Salens, W.; Feremans, G.; Segher, K.; François, S. Anomaly detection in long-term tunnel deformation monitoring. *Eng. Struct.* **2022**, *250*, 113383. [CrossRef]
23. Liu, H.; Zhang, Z.L.; Zhang, Z.B.; Sun, M.L.; Liu, Z.C. Study on evaluation method of construction disturbance for twin single-line metro tunnel undercrossing existing tunnel. *Railw. Stand. Des.* **2024**, *68*, 149–157. [CrossRef]
24. Li, S.C.; Liu, B.; Sun, H.F.; Nie, L.C.; Zhong, S.H.; Su, M.X.; Li, X.; Xu, Z.H. State of art and trends of advanced geological prediction in tunnel construction. *Chin. J. Rock. Mech. Eng.* **2014**, *33*, 1090–1113.
25. Liang, F.Y.; Yuan, Q.; Li, J.P.; Zhang, S.X. Influences of soil characteristics on longitudinal deformation of shield tunnels induced by surface surcharge. *Chin. J. Geotech. Eng.* **2020**, *42*, 63–71. [CrossRef]
26. Clough, G.W. Construction Induced movements of in situ wall, design and performance of earth retaining structure. In Proceedings of the ASCE Design and Performance of Earth Retaining Structures, Ithaca, NY, USA, 18–21 June 1990; pp. 439–479.
27. Yang, C.; Huang, R.; Liu, D.; Qiu, W.; Zhang, R.; Tang, Y. Analysis and warning prediction of tunnel deformation based on multifractal theory. *Fractal Fract.* **2024**, *8*, 108. [CrossRef]
28. Liu, L.K. Technical scheme of safety monitoring system for urban rail transit operating environment. *Int. J. Syst. Assur. Eng. Manag.* **2023**, *14*, 635–647. [CrossRef]
29. Wei, G.; Feng, W.H.; Wu, X.H.; Li, H.; Zhu, Z.Y.; Wang, Z. Research on the combined control of tunnel deformation adjacent to the foundation pit by servo steel strut and capsule grouting. *Sci. Rep.* **2025**, *15*, 23432. [CrossRef] [PubMed]

30. Chen, B.G.; Yan, T.F.; Song, D.H.; Luo, R.P.; Zhang, G.H. Experimental investigations on a deep excavation support system with adjustable strut length. *Tunn. Undergr. Space Technol.* **2021**, *115*, 104046. [CrossRef]
31. Di, H.G.; Jin, Y.Y.; Zhou, S.H.; Zhang, X.H.; Wu, D.; Guo, H.J. Experimental study on the adjustments of servo steel struts in deep excavations. *Acta Geotech.* **2023**, *18*, 6615–6629. [CrossRef]